LAWRENCE
LIVERMORE
NATIONAL
LABORATORY

LLNL-PROC-402915

Ion Exclusion by Sub 2-nm Carbon Nanotube Pores

F. Fornasiero, H. G. Park, J. K. Holt, M. Stadermann, C. P. Grigoropoulos, A. Noy, O. Bakajin

April 14, 2008

MRS Meeting Spring 2008
San Francisco, CA, United States
March 24, 2008 through March 28, 2008

Disclaimer

LLNL-PROC-402915

Ion Exclusion by sub 2-nm Carbon Nanotube Pores

Francesco Fornasiero[*], Hyung Gyu Park[*], Jason K Holt[*], Michael Stadermann[*], Costas P. Grigoropoulos[†], Aleksandr Noy[*‡], and Olgica Bakajin[*§]

[*] Biosciences and Biotechnology Division, Chemistry Materials Earth and Life Sciences, Lawrence Livermore National Laboratory, Livermore CA 94550

[†] Department of Mechanical Engineering, University of California at Berkeley, Berkeley CA 94720

[‡] School of Natural Sciences, University of California at Merced, Merced CA 95344

[§] NSF Center for Biophotonics Science & Technology, University of California at Davis, Sacramento CA 95817

ABSTRACT

Carbon nanotubes offer an outstanding platform for studying molecular transport at nanoscale, and have become promising materials for nanofluidics and membrane technology due to their unique combination of physical, chemical, mechanical, and electronic properties. In particular, both simulations and experiments have proved that fluid flow through carbon nanotubes of nanometer size diameter is exceptionally fast compared to what continuum hydrodynamic theories would predict when applied on this length scale, and also, compared to conventional membranes with pores of similar size, such as zeolites.

For a variety of applications such as separation technology, molecular sensing, drug delivery, and biomimetics, selectivity is required together with fast flow. In particular, for water desalination, coupling the enhancement of the water flux with selective ion transport could drastically reduce the cost of brackish and seawater desalting. In this work, we study the ion selectivity of membranes made of aligned double-walled carbon nanotubes with sub-2 nm diameter. Negatively charged groups are introduced at the opening of the carbon nanotubes by oxygen plasma treatment.

Reverse osmosis experiments coupled with capillary electrophoresis analysis of permeate and feed show significant anion and cation rejection. Ion exclusion declines by increasing ionic strength (concentration) of the feed and by lowering solution pH; also, the highest rejection is observed for the $A_m^{z_A}C_n^{z_C}$ salts (A=anion, C=cation, z= valence) with the greatest z_A/z_C ratio. Our results strongly support a Donnan-type rejection mechanism, dominated by electrostatic interactions between fixed membrane charges and mobile ions, while steric and hydrodynamic effects appear to be less important. Comparison with commercial nanofiltration membranes for water softening reveals that our carbon nanotube membranes provides far superior water fluxes for similar ion rejection capabilities.

INTRODUCTION

In the last few years, fluid transport through carbon nanotubes has been subject of intense theoretical and experimental research [1]. MD simulations performed by G. Hummer and colleagues revealed an unexpected effect: they found that water molecules spontaneously fill a (6,6) carbon nanotube (0.81 nm in diameter and 1.34 nm in length) [2]. Several experimental studies also provided some evidence of water filling of carbon nanotubes [3-6]. Several MD simulations also demonstrated extremely high transport rates of water through CNTs [2,7,8]. Weak interactions of water molecules with the hydrophobic walls combine with the smooth nature of the nanotube walls to enable nearly-frictionless, ultrafast transport of water in nanotubes channels [8].

Recently, extremely high, pressure-driven flow-rates of water have been reported through sub-2-nm DWNT membranes [9] and through MWNT membranes with larger pore diameters [10]. Measured flow rates correspond to enhancements of 4–5 orders of magnitude compared with the no-slip, hydrodynamic flow calculated using the Hagen–Poiseuille equation for MWNT membranes [10], and of at least 2–3 orders of magnitude for DWNT membranes [9]. Experimental water fluxes compare well with those predicted by MD simulations. With 100-atm osmotic pressure, ~12 water molecules flow through a CNT per nm^2 of cross-sectional area per ns [11]. Measured fluxes, extrapolated to the simulation pressure drop, correspond to 10–40 water molecules per nm^2 per ns [9].

Applications of membranes for molecular separations require selectivity together with fast flow. In particular, for water desalination, coupling the enhancement of the water flux with selective ion transport could drastically reduce the cost of brackish and seawater desalting. Molecular dynamics simulations of salt-solution pressure-driven flow suggest that uncharged CNT with 0.8 nm diameter can efficiently exclude ions while maintaining ultrafast water flow [7,12].

So far only one experimental study investigated ion transport/exclusion though narrow (< 5 nm) CNT pores [13]. In this work [13], we studied the ion exclusion properties of DWNT with sub-2-nm diameter CNTs whose entrance is decorated by negatively charged carboxylic groups. These DWNT span the whole thickness of an otherwise impermeable silicon nitride (SiN_x) membrane. We used pressure to drive the filtration of ionic solutions through the SiN_x /CNT composite membranes. Ionic content of both feed and permeate was measured using capillary electrophoresis or UV spectroscopy. We summarize here our findings from this previous work [13].

EXPERIMENT

Membrane Fabrication

SiN_x/CNT composite membranes are fabricated as explained elsewhere [9]. Briefly, a vertically aligned array of CNTs in encapsulated with low-stress SiN_x by an extremely conformal, low pressure CVD process. After encapsulation, the membrane undergoes a series of etching steps to remove excess SiN_x from the tips of the CNTs, followed by oxygen plasma to uncap the CNTs. The resulting free standing membrane is located in 89 windows (50 μm in diameter) etched on a silicon support (Figure 1) [9]. TEM of thinned-down sections of our

double-walled CNT (DWNT) membranes shows pores with less than 2 nm in diameter, consistent with diameters of as-grown nanotubes. The absence of nano - or microvoids larger than the nanotube diameter is also demonstrated by the full retention of 2 nm gold nanoparticles during filtration of colloidal gold solution [9].

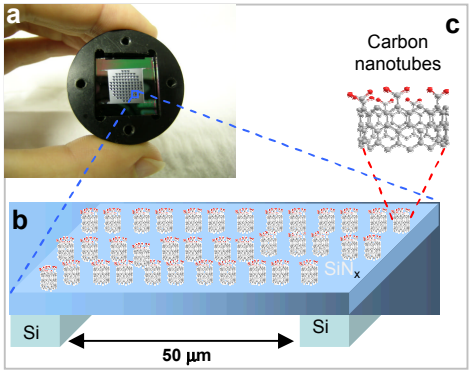

Figure 1. Silicon nitride - carbon nanotube membrane. a) Picture of the permeate side of a SiN_x/carbon nanotube platform showing the 89 windows where the free standing membrane resides; b) schematic representation of a 50 µm window containing the free standing SiN_x/carbon nanotube membrane; c) schematic of the carbon nanotube rim decorated by carboxylic groups.

Nanofiltration

Figure 2 shows a schematic of the nanofiltration set-up. A CNT membrane is mounted in a filtration cell so that it divides the cell in two chambers. The top chamber (feed) is filled with about 2 ml of salt solution. The feed solution is pressurized at 0.69 bar, while the permeate chamber is kept at atmospheric pressure. Permeate flow rate is recorded as variation of the column height of the feed solution with respect to time.

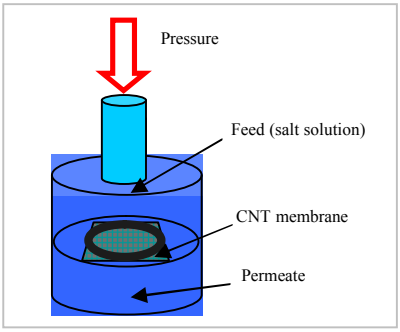

Figure 2. Schematic representation of the experimental nanofiltration cell

At the end of a nanofiltration experiment, solution samples from both feed and permeate are collected and analyzed by either capillary electrophoresis (Hewlett Packard 3D CE capillary electrophoresis system, Agilent Technologies, Santa Clara, CA) or UV-vis spectroscopy (PerkinElmer, Waltham, MA). The rejection coefficient R for an ion i is calculated as:

$$R = 1 - \frac{c_i^p}{c_i^f} \quad (1)$$

where c_i^f and c_i^p, are the ion concentrations in the feed and permeate, respectively. More details on the experimental methods are reported in Reference [13].

DISCUSSION

Ultrafast flow and electrolyte exclusion

Capillary electrophoresis (CE) analysis of the ion concentration before and after nanofiltration shows that the DWNT membranes exclude a large part of the feed solution ionic content. Moreover, carbon nanotube membranes maintain the ultrafast rates of water flow reported in our previous study [9]. For example, filtration of 1.0 mM potassium ferricyanide solution under an applied pressure of 0.69 bar results in the exclusion of ~90% of the original ions. For 1.0 mM potassium chloride solution under 0.69 bar, the rejection is about 40%. These rejection ratios are comparable to the rejection ratios exhibited by a tight nanofiltration membrane tested under the same conditions. Note that our DWNT membranes provide an order of magnitude higher flux than the tested commercial nanofiltration membrane.

Effect of solution pH

To test if electrostatic interactions are an important determinant of the ion exclusion in silicon nitride/ sub-2-nm CNT composite membranes, we study ion rejection as a function of solution pH. The carbon nanotube rims are decorated by carboxylic groups because of the etching processes used to expose and open the carbon nanotubes [14,15]. For a feed solution pH larger than the carboxylic acid pK_a (~ 4.5 on a CNT [16,17]), these groups are fully ionized and electrostatic forces may affect ion transport through the nanotube channels. On the opposite, for a solution pH smaller than the carboxylic acid pK_a, the carboxylic groups become protonated and electrostatic contributions to the mechanism of ion exclusion are effectively turned off.

For these experiments we used a 0.5mM solution of pyrene tetrasulfonic sodium salt. For the same ionic strength, a decrease of the feed pH from 7.2 to 3.8 results in a significant decrease of the measured rejection coefficient (from 96% at pH=7.2 to 60% at pH=3.8) [13]. These experimental observations indicate that the electrostatic forces between carboxylic groups on the CNT rim and the free ions play a significant role in the rejection of electrolytes during salt solution nanofiltration.

Effect of ion valence

Nanofiltration of solution of ions of different valences was used to further understand the underlying mechanism of ion exclusion. For this study, dilute solutions of the following salts were prepared at the same equivalent concentration (1mM): $K_3Fe(CN)_6$ (cation-anion valence, z_A-z_C: 1-3), K_2SO_4 (1-2), $CaSO_4$ (2-2), KCl (1-1), $CaCl_2$(2-1), and $Ru(bipy)_3 \cdot Cl_2$ (2-1) (tris(2,2'-bipyridyl)dichlororuthenium hexahydrate). Properties of these ions are reported in Table I.

Experimentally measured rejection coefficients were compared with the prediction of the Donnan theory.

Table I. Studied ionic species: valence z, hydrated radius r_h, and Stokes radius r_s. Reported hydrated radii are from Reference [18], except for $Fe(CN)_6^{3-}$ (crystallographic radius [19]) and $Ru(bipy)_3^{2+}$ [20].

Ion	z	r_h [nm]	r_s [nm]
$Fe(CN)_6^{3-}$	-3	0.475	0.273
SO_4^{2-}	-2	0.379	0.230
Cl^-	-1	0.332	0.121
K^+	1	0.331	0.125
Ca^{2+}	2	0.412	0.310
$Ru(bipy)_3^{2+}$	2	0.590	0.475

The Donnan model provides a well-known classical description of the electrochemical equilibrium that is established when an ionic solution contacts a charged membrane. The theory treats ions as point charges; thus, it neglects ion size effects, while accounting for electrostatic interactions. According to the Donnan theory, for the same membrane fixed charge, the rejection coefficient of salt solutions with identical equivalent concentration depends only on the ratio of the anion and cation valence:

$$R = 1 - \frac{c_A^m}{c_A} = 1 - \left(\frac{|z_A| c_A}{|z_A| c_A^m + c_x^m} \right)^{|z_A/z_C|} \qquad (2)$$

where c_A and c_A^m, are the concentrations of co-ions (anions here) in the solution and in the membrane phase respectively, c_x^m is the membrane charge concentration, z is the ion valence, and subscripts A and C indicate co-ions (anions) and counter-ions (cations), respectively.

The highest rejection (~90%) was indeed measured for the $A_m^{z_A} C_n^{z_C}$ salts with the greatest z_A/z_C ratio ($K_3Fe(CN)_6$) followed by K_2SO_4, $CaSO_4$, KCl, $CaCl_2$, and $Ru(bipy)_3 \cdot Cl_2$. Our results are, therefore, in a close agreement with the prediction of the Donnan membrane equilibrium theory (Figure 3). Interestingly, the biggest ions considered in this series ($Ru(bipy)_3 \cdot Cl_2$) can permeate almost freely through the membrane because its z_A/z_C ratio is only 0.5. Thus, this trend strongly supports a rejection mechanism dominated by electrostatic interactions between fixed membrane charges and mobile ions [13]. On the opposite, steric and hydrodynamic effects appear to be less important [13].

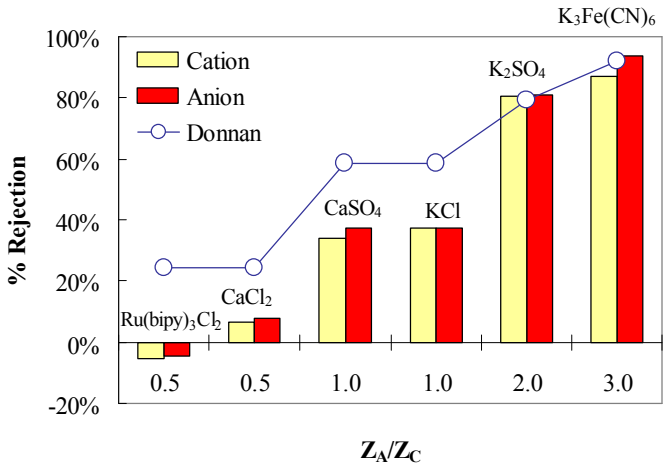

Figure 3. Rejection coefficients (bars) measured for six salt solutions that have the same equivalent concentration but different ion valence. Points (filled circles) indicate rejections calculated with the Donnan theory, Eq. 2, with a membrane charge density c_x^m=2.0 mM (this value was chosen to fit $K_3Fe(CN)_6$ rejection). This density corresponds to about 7 charged groups per nanotube [13].

Effect of ionic strength

Previous experiments consider very dilute salt solutions (<1mM). To further characterize the performance of our membranes, we measured the rejection coefficient as a function of the solution concentration. We increased salt concentration more than 2-orders of magnitude (from 0.1 to 12 mM for $K_3Fe(CN)_6$ and from 0.3 mM to 36 mM for KCl). For $K_3Fe(CN)_6$, rejection decreased from almost complete exclusion to negligible exclusion by increasing salt concentration. A similar trend was observed for KCl, for which the highest measured rejection was ~ 50% [13]. This trend is also consistent with a mechanism of ion exclusion dominated by electrostatic interaction. An increase of the salt concentration effectively screens electrostatic forces and, thus, reduces ion rejection. A second concomitant mechanism may be partially responsible for the observed trend. Because the applied pressure is constant at all solution concentrations, an increase of salt concentration corresponds to a reduced driving force for water transport and an increased driving force for ion transport. Thus, even for uncharged solutes, an increase of salt concentration may induce a reduction of the measured rejection.

CONCLUSIONS

We have used pressure-driven nanofiltration of ionic solutions through sub 2-nm carbon nanotube membranes to study ion rejection by carbon nanotubes that have carboxylic groups on their rim. Analysis of ion concentration in the feed and permeate reveals that these membranes are able to significantly reject small ions at low solution concentrations while maintaining ultrafast water transport rates. Further improvement of membrane performance at higher solution concentration may be potentially achieved by increasing the membrane charge density and / or by reducing the CNT pore size.

ACKNOWLEDGMENTS

This work was partially supported by Defense Advanced Research Projects Agency DSO & Lawrence Livermore National Laboratory. This work performed under the auspices of the U.S. Department of Energy by Lawrence Livermore National Laboratory under Contract DE-AC52-07NA27344. CG & OB were partially supported by NSF NER 0608964. AN, CG, OB, SK &JBI acknowledge support by NSF NIRT CBET-0709090. OB also acknowledges support by the Center for Biophotonics, an NSF Science and Technology Center, managed by the University of California, Davis, under Cooperative Agreement PHY 0120999. The authors thank Gregory L. Klunder for advises regarding the capillary electrophoresis analysis, and Matthew D. Hamtak for help in the experimental work.

REFERENCES

1. A. Noy; H. G. Park; F. Fornasiero; J. K. Holt; C. P. Grigoropoulos; O. Bakajin. *Nano Today* 2007, 2, **22-29** (2007).
2. G. Hummer; J. C. Rasaiah; J. P. Noworyta. *Nature* 2001, 414, **188-190** (2001).
3. A. I. Kolesnikov; J. M. Zanotti; C. K. Loong; P. Thiyagarajan; A. P. Moravsky; R. O. Loutfy; C. J. Burnham. *Phys Rev Lett* 2004, 93, **35503** (2004).
4. N. Naguib; H. Ye; Y. Gogotsi; A. G. Yazicioglu; C. M. Megaridis; M. Yoshimura. *Nano Lett* 2004, 4, **2237–2243** (2004).
5. Y. Maniwa; K. Matsuda; H. Kyakuno; S. Ogasawara; T. Hibi; H. Kadowaki; S. Suzuki; Y. Achiba; H. Kataura. *Nature Mater* 2007, 6, **135-141** (2007).
6. E. Mamontov; C. J. Burnham; S. H. Chen; A. P. Moravsky; C. K. Loong; N. R. de Souza; A. I. Kolesnikov. *J Chem Phys* 2006, 124, **194703** (2006).
7. C. Corry. *J Phys Chem B* 2008, 112, **1427-1434** (2008).
8. S. Joseph; N. R. Aluru. *Nano Lett* 2008, 8, **452-458** (2008).
9. J. K. Holt; H. G. Park; Y. M. Wang; M. Stadermann; A. B. Artyukhin; C. P. Grigoropoulos; A. Noy; O. Bakajin. *Science* 2006, 312, **1034-1037** (2006).
10. M. Majumder; N. Chopra; R. Andrews; B. J. Hinds. *Nature* 2005, 438, **44-44** (2005).
11. A. Kalra, Garde, S. & Hummer, G. *Proc Natl Acad Sci USA* 2003, 100, **10175-10180** (2003).
12. M. E. Suk; A. V. Raghunathan; N. R. Aluru. AIP, 2008, p 133120.
13. F. Fornasiero; H. G. Park; J. K. Holt; M. Stadermann; C. P. Grigoropoulos; A. Noy; O. Bakajin. *Proc Natl Acad Sci USA* 2008, in press (2008).
14. D. Q. Yang; J. F. Rochette; E. Sacher. *Langmuir* 2005, 21, **8539-8545** (2005).
15. P. H. Li; X. D. Lim; Y. W. Zhu; T. Yu; C. K. Ong; Z. X. Shen; A. T. S. Wee; C. H. Sow. *J Phys Chem B* 2007, 111, **1672-1678** (2007).
16. S. S. Wong; A. T. Woolley; E. Joselevich; C. L. Cheung; C. M. Lieber. *J Am Chem Soc* 1998, 120, **8557-8558** (1998).
17. S. S. Wong; E. Joselevich; A. T. Woolley; C. L. Cheung; C. M. Lieber. *Nature* 1998, 394, **52-55** (1998).
18. E. R. Nightingale. *J Phys Chem* 1959, 63, **1381-1387** (1959).
19. D. J. Carter; M. I. Ogden; A. L. Rohl; Yz. *Aust J Chem* 2003, 56, **675-678** (2003).
20. M. Majumder; N. Chopra; B. J. Hinds. *J Am Chem Soc* 2005, 127, **9062-9070** (2005).